Original Article
Journal of Biosystems Engineering

J. of Biosystems Eng. 40(3):250-260. (2015. 9)
http://dx.doi.org/10.5307/JBE.2015.40.3.250

eISSN : 2234-1862
pISSN : 1738-1266

Design and Fabrication of a Dual Cylindrical Microwave and Ohmic Combination Heater for Processing of Particulate Foods

Seung Hyun Lee[1], Won Choi[2], Sung Hee Park[3], Soojin Jun[3]*

[1]*Department of Biosystems Machinery Engineering, Chungnam National University, 220 Gung-Dong, Yuseong-Gu, Daejeon, 305-764, South Korea*
[2]*Department of Rural Systems Engineering, Seoul National University, Seoul 151-921, South Korea*
[3]*Department of Human Nutrition, Food and Animal Sciences, University of Hawaii, Honolulu, HI 96822, USA*

Received: August 10th, 2015; Revised: August 20th, 2015; Accepted: August 24th, 2015

Abstract

Purpose: Dual cylindrical microwave chambers equipped with an ohmic heating tube were designed and fabricated to maximize the electric field strength for expeditious heat treatment of particulate foods. **Methods:** The efficacy of the combination heater was investigated by simulating the electric field distribution by using COMSOL Multiphysics software. **Results:** All components of the designed microwave heating unit were suitable for transmitting maximal microwave power to the load. The simulated electric field distribution implied that single-mode microwave heating would be sufficient for the steady generation of a highly localized heating zone in the cavity. During impedance matching, the calculated reflection coefficient (S_{11}) was small, possibly implying minimal power loss and wave reflection in the designed microwave heating chamber. **Conclusions:** This study demonstrates the possibility of concentrating the microwave power at the centerline for a single-frequency microwave, for thermal treatment of multiphase foods without attenuating the microwave power.

Keywords: 3D simulation, Combination heating, Electric field distribution, Microwave, Ohmic heating

Introduction

Microwave technology has been utilized in a wide range of fields, including communication systems, radar systems, and medical systems (Pozar, 2005). Microwaves (MW), which are a part of the electromagnetic spectrum occupying the 300 MHz to 300 GHz frequency band, have been extensively used in various stages of food processing, such as drying, tempering, and cooking, because microwaves allow rapid and direct heating of food (Lee and Jun, 2011). In particular, the domestic microwave oven has become the most useful home appliance because of its simple operation and ability to rapidly heat or thaw frozen foods. However, the microwave power intensity of the domestic microwave oven (the typical example of a multi-mode microwave cavity) is not evenly distributed in the target food material, resulting in non-uniform intra-food heating (Barlow and Marder, 2003). Several factors that affect heating uniformity in food materials during microwave heating, i.e., the dielectric properties, volume, geometry, and shape of the food materials, have been investigated (Anantheswaran and Liu, 1994). However, there is a dearth of studies concerning the design and geometric parameters of microwave resonant cavities for processing food products.

Microwave cavity resonators for food processing can be classified into two common types: single-mode and multimode. The presence of different resonance modes can consequentially lead to multiple hot spots apparently disconnected in the multimode cavity (Bradshaw et al., 1998). The multimode cavity is versatile for thermal processing of various food materials that have large volume, complicated shape, and different dielectric properties (Das et al., 2008).

***Corresponding author:** Soojin Jun
Tel: +1-808-956-8283; **Fax:** +1-808-956-4026
E-mail: soojin@hawaii.edu

In general, several fundamental standing modes can be generated in the cavity; however, it is not guaranteed that all resonance modes will be generated and excited, which causes non-uniform temperature distribution in the food product undergoing microwave heating (Chan and Reader, 2000). The practical approaches to increase thermal uniformity in a multimode cavity have been explored by a number of researchers. Tang et al. (2008) reported that using a magnetron with higher frequency (5.8 GHz) could increase the power density and processing efficiency fourfold, compared with the conventional 2.45 GHz magnetron. Another advantageous approach for a multimode cavity with fixed dimensionality is to install multiple microwave feeding ports (magnetrons or power inputs) in the cavity (Tran, 1992). However, the suggested approaches require supplementary equipment, i.e., a mode stirrer that is closely associated with the heating patterns of food materials and microwave leakage. In addition, achieving critical and detail design of the multimode cavity is time-consuming.

On the other hand, a single-mode cavity resonator was designed and exploited to support only one standing wave at the source frequency (Sun et al., 2005). Single-mode cavities have been intensively used for heat treatment of food products with a limited volume and weak dielectric properties, owing to the existence of only one hot spot with well-defined electric field pattern (Kybartas et al., 2011).

Single-mode cavity resonators are most commonly designed to have rectangular or cylindrical shapes. A rectangular cavity resonator can be simply made from a rectangular waveguide by shorting both ends with a metal plate (Chan and Reader, 2000). However, a cylindrical cavity usually has higher quality factor (Q), implying smaller microwave energy loss for a cavity resonator compared with a rectangular cavity; thus, it is possible to achieve a highly localized heating zone at the central axis of a cylindrical cavity resonator. Cylindrical single-mode microwave cavities can be used for continuous-flow thermal processing with constant electric field strength (Chen et al., 2004).

In addition, the design of an ohmic heater with pulsed square waveforms at higher frequencies and the use of chemically inert materials for electrodes have made this technique more reliable and commercially successful. However, when ohmic heating is applied for the processing of multiphase foods, the different heating rates of solids and liquids are frequently observed owing to the different electrical conductivities of particles and liquids. The different heating rates can result in the generation of under-processed particulates. Therefore, separate pretreatment steps for particulate and liquid foods are necessary to equilibrate the electrical conductivities of particle and liquid foods (Nguyen et al., 2013). To remove the required pretreatment step in the thermal treatment of multiphase foods, a combined microwave and ohmic heater has been developed for the processing of multiphase foods. It will be technically feasible to obtain thermal uniformity in multiphase foods by using the developed microwave and ohmic combination heater, because solid particles and liquid are simultaneously heat-treated by electric currents and electromagnetic waves, depending on their dielectric properties. This study was aimed at the design and fabrication of a dual cylindrical microwave and ohmic combination heater for the processing of particulate foods.

Materials and Methods

Model development

The majority of the existing microwave heating systems are mainly composed of a microwave power source (magnetron that generates the electromagnetic radiation), the transmission line (waveguides that deliver high electromagnetic power from the power source to the cavity and can be considered as conductors), and the cavity resonator (rectangular or cylindrical cavity resonator) (Chan and Reader, 2000). The electric and magnetic field distributions in a microwave heating system can be numerically analyzed by using Maxwell's equations. Furthermore, the design parameters associated with the transmission line and the cavity resonator may be easily derived from Maxwell's equations (Zhao et al., 2011):

$$\nabla \times E = j\omega\mu_0 H, \nabla \times H = j\omega\varepsilon_0\mu_0 H, \nabla \cdot E = 0, \nabla \cdot H = 0 \quad (1)$$

where E is the electric field (V/m), H is the magnetic field (A/m), ω is the angular velocity (rad/s), μ_0 is the vacuum permeability (1.25664×10^{-7} H/m), and ε_0 is the vacuum dielectric constant (8.854×10^{-12} F/m).

The rate of ohmic heating is the product of the square of the applied electric field strength and the food electrical conductivity. In particular, the electrical conductivity of a

food linearly depends on its temperature, and can be estimated from the following equation (Shim et al., 2010);

$$\sigma = \frac{I}{V} \cdot \frac{L}{A} \tag{2}$$

where V is the applied voltage (V), σ is the electrical conductivity (S/m), I is the current (A), L is the distance between the electrodes (m), and A is the contact area (m^2).

Temperature distribution inside the food subject to ohmic heating is:

$$\rho C_p \frac{\partial T}{\partial t} = \nabla (k \nabla T) + U \tag{3}$$

where ρ is the food density (kg/m^3), C_p is the food specific heat (J/kg K), t is the time (s), k is the food thermal conductivity (W/m K), T is the food temperature (K), and U is the internal energy source.

The internal energy source of ohmic heating is given by (Shim et al., 2010):

$$U = \sigma(T) |\nabla V|^2 \tag{4}$$

In addition, the electric field distribution in an ohmic heating applicator can be defined by Laplace's equation (De Alwis and Fryer, 1990):

$$\nabla [\sigma(T) \nabla V] = 0 \tag{5}$$

Rectangular waveguide

Waveguides can be produced to have various shapes, most commonly rectangular or cylindrical shapes. Rectangular waveguides have been used in microwave heating systems owing to the efficient microwave energy transmission from the microwave power source to the cavity resonator (Rattanadecho et al., 2008; Cha-um et al., 2009). Standard rectangular waveguides have aspect ratios close to 2:1 (width:height) and the waveguide size depends on the frequency range; however, for specific purposes, reduced-height waveguides can sometimes be used (Cooper and Carter, 1991). Standard WR430 or WR340 can be utilized in microwave heating systems powered by the magnetron at 2.45 GHz.

According to the particular geometry of a microwave waveguide, only specific patterns of electric and magnetic fields, which are also known as modes, can exist as propagating waves. The allowed propagation modes within a waveguide can be determined from dominant components (Mekis et al., 1996). Transverse electric (TE) and transverse magnetic (TM) modes in rectangular or cylindrical waveguides can be determined by the cutoff frequency (f_c), below which all frequencies in the waveguide are attenuated. Above the cutoff frequency, microwave power can be transferred from the source to the cavity without attenuation. The TE modes dominate in rectangular waveguides and are usually expressed as TE_{mn} (m and n denote half-wavelength variations in the field strength in the horizontal and longitudinal directions, respectively, of the rectangular waveguide). The dominant mode, which has the lowest cutoff frequency and the lowest order of m and n in the waveguide, is the TE_{10} mode (Pozar, 2005). Because all transverse field components (E_x, E_y, H_x, and H_y) are zero (no wave propagation in the waveguide) when m and n in the TE_{mn} mode are zero, the TE_{00} mode does not exist in the waveguide (Elashafiey, 2011). To estimate all of the transverse field components in the TE_{mn} mode, the propagation constant (β) should be calculated from the following equation:

$$\beta = \sqrt{k^2 - \left(\frac{m\pi}{a}\right)^2 - \left(\frac{n\pi}{b}\right)^2}, k = \omega\sqrt{\mu\varepsilon} \tag{6}$$

where k is the medium wave number, μ is the medium permeability (H/m), ε is the medium dielectric constant (F/m), a and b are either the width (m) and height (m) of a rectangular waveguide or the radius (m) and height (m) of a cylindrical waveguide, respectively.

The cutoff frequency (f_c) of the TE_{mn} mode is:

$$f_c = \frac{c}{2\pi\sqrt{\mu\varepsilon}} \sqrt{\left(\frac{m\pi}{a}\right)^2 + \left(\frac{n\mu}{b}\right)^2} \tag{7}$$

where c is the speed of light in vacuum (2.998×10^8 m/s).

For the TE_{10} mode, the cutoff frequency can be expressed as $\frac{c}{2a\sqrt{\mu\varepsilon}}$ or $\frac{c}{2a\sqrt{\varepsilon_r}}$ (ε_r is the relative dielectric constant of the waveguide material).

The guide wavelength (λ_g), the distance between two equal phase planes along the waveguide, can be used in the design of the distributed electric (E) and magnetic (M) field structures (Veronis and Fan, 2005). It is also a function of the lower cutoff wavelength and has a longer wavelength than the wavelength ($\lambda = \frac{c}{f}$) in vacuum. The guide wavelength (λ_g) can be determined by:

$$\lambda_{guide} = \frac{2\pi}{\beta} \tag{8}$$

Cylindrical cavity resonator

Similar to the single-mode rectangular cavity resonator, a single-mode cylindrical cavity resonator can be built from a cylindrical waveguide by sealing both ends with metal. In the cylindrical cavity resonator, the dominant TE mode is the TE_{11} mode (Pozar, 2005). By combining a cylindrical cavity resonator and a rectangular waveguide, the desirable field strength distribution at specific locations inside the cavity can be obtained and the heating direction in the cavity can be adjusted (Tang et al., 2008).

The propagation constant (β) of the TE_{nm} mode can be derived from Eq. (6). The values of p'_{nm} for the TE_{nm} mode, which can affect the direction of wave propagation in a microwave cavity resonator, are shown in Table 1. Furthermore, m and n refer to the number of variations at the standing wave pattern in the x and y directions inside the cavity (Pozar, 2005). The propagation constant is:

$$\beta = \sqrt{k^2 - \left(\frac{p'nm}{a}\right)^2} \tag{9}$$

where a is the radius of the cylindrical cavity resonator.

Then, the cutoff frequency (f_c) of the TE_{nm} mode is:

$$f_c = \frac{cp'_{nm}}{2\pi a\sqrt{\mu\varepsilon}} \tag{10}$$

The resonant frequency (f_r) is a key factor that determines the dimension of the cavity and filling materials (Hardy and Whitehead, 1981). The parameter l in Eq. (11) refers to the number of variations in the standing wave pattern in the z direction inside the cavity (Pozar, 2005). It can be calculated by using the following equation:

$$f_r = \frac{c}{2\pi\sqrt{\mu\varepsilon}}\sqrt{\left(\frac{p'_{nm}}{a}\right)^2 + \left(\frac{l\pi}{b}\right)^2} \tag{11}$$

Table 1. The values of p_{nm} for the TE_{nm} mode in the cylindrical cavity resonator

n	p'_{n1}	p'_{n2}	p'_{n3}
0	3.832	7.016	10.174
1	1.841	5.311	8.536
2	3.054	6.706	9.970

Impedance matching

During the design of a microwave heater, impedance matching is an essential procedure to ensure that maximal microwave power is transmitted and wave reflection is minimized (Pozar, 2005). In addition, while electromagnetic waves travel down the waveguide, generation of currents that may cause ohmic loss and gradual wave attenuation should be prevented by impedance matching (Chan and Reader, 2000). Several types of impedance matching have been introduced, such as matching with lumped elements or single, double, and series stub matching. The series stub matching method was used in this study owing to its practicality and convenience for designing microwave heating systems (Berliner and Bender, 2004). A stub is an open or short circuit transmission line connected either in parallel or in series with the transmission feed line; therefore, by adjusting the location of stubs on a waveguide with a certain distance from the load, microwaves can be made to pass through the central axis of the cylindrical cavity where the load is placed (Torungrueng and Thimaporn, 2004). In a general design of a microwave heating system, the distance between series of stubs can be $\lambda_g/3$, $\lambda_g/6$, or $\lambda_g/4$, where λ_g is the guide wavelength.

Impedance matching for a microwave heating system

A microwave dummy probe connected to a vector network analyzer (VNA, N9923A, Agilent Technologies, Santa Clara, CA) was used to measure the scattering parameter (S_{11}, the reflection coefficient). Before impedance matching, the probe was calibrated with open and short circuits and the matched load, which had the characteristic impedance (Z_0) of 50 Ω. The S_{11} value was close to 50 Ω at the center of the Smith chart, which stands for minimal wave reflection; this value was obtained by controlling the locations and lengths of 5 matching stub towers on the top surface of the custom-designed waveguide.

Results and Discussion

Microwave power launcher

The dimensions of a microwave power launcher can be determined by using a microwave power source operating at a certain frequency. US Federal Communication Commission (FCC) allocated four frequencies (915 MHz, 2.45,

5.8, and 24.15 GHz) for industrial, scientific, and medical (ISM) applications (Roussy and Pearce, 1998). Magnetrons operating at 915 MHz and 2.45 GHz for microwave heating have been commonly used as the microwave energy sources. Furthermore, magnetrons at 2.45 GHz have been intensively used for small and laboratory scale applications because of their high energy efficiency and low cost (Chan and Reader, 2000). A microwave power launcher with 2.45 GHz can be fabricated by using the WR430 rectangular waveguide with the cutoff frequency of 1.37 GHz at the TE_{10} mode. Although a standard size of the WR430 waveguide is recommended for a simple design of a microwave power launcher operating in the 1.7 to 2.6 GHz frequency range, the modified WR430 waveguide with reduced frequency bandwidth can be utilized for maximal microwave power transfer to the load (Wheeler et al., 2002). The modified WR430 waveguide, with dimensions of 95.3 mm (width), 54.6 mm (height), and 159 mm (length), was designed for the microwave power launcher. A magnetron operating at 2.45 GHz (Model OM75S, Samsung) was used as a microwave power source. Using the width (95.3 mm) and height (54.6 mm) of the microwave power launcher and the frequency of 2.45 GHz in the TE_{10} mode, the calculated propagation constant (β), cutoff frequency (f_{c10}), and guide wavelength (λ_g), obtained from Eqs. (6), (7), and (8), were 39.52, 1.57 GHz, and 0.159 m, respectively. The length of the launcher was the same as the calculated guide wavelength (λ_g). The distance between the output antenna of the magnetron and the right end of the launcher was 148 mm, same as the guide wavelength (λ_g) of the WR430 waveguide, corresponding to the frequency of 2.45 GHz in the TE_{10} mode. The launcher was built from nickel-coated brass.

Cylindrical microwave cavity resonator

A cylindrical cavity resonator, coupled with the WR430 rectangular waveguide operating in the TE_{10} mode, was designed in the axis-symmetric TE_{111} mode (Figure 1).

The calculated cutoff frequency (f_c) of the WR430 rectangular waveguide was 1.372 GHz. In order to match the cutoff frequencies of the rectangular waveguide and the cylindrical cavity, the radius of the cylindrical cavity was determined by using Eq. (7), which can also be used for a cylindrical microwave cavity. The diameter of the designed cylindrical cavity was 127 mm, a little longer than the wavelength for 2.40 GHz (λ = 125 mm), because the frequency resolution of the magnetron operating at 2.45 GHz was ± 0.05 GHz and damage to the magnetron can be prevented by making the diameter slightly larger than the wavelength associated with the magnetron resolution frequency. The distance between the center of the cylindrical cavity and the waveguide end was 125 mm, corresponding to the wavelength associated with the frequency of 2.40 GHz; while approximately half of the guide wavelength at 2.40 GHz, (λ_g = 80 mm), was applied toward the length of the rectangular waveguide for efficient coupling of the rectangular waveguide and the cylindrical cavity (Sreekanth, 2003). When the rectangular waveguide (109.2 × 54.6 × 80 mm^3, W × H × L) was considered as the rectangular cavity resonator operating at 2.45 GHz in the TE_{101} mode that exhibits no variation in

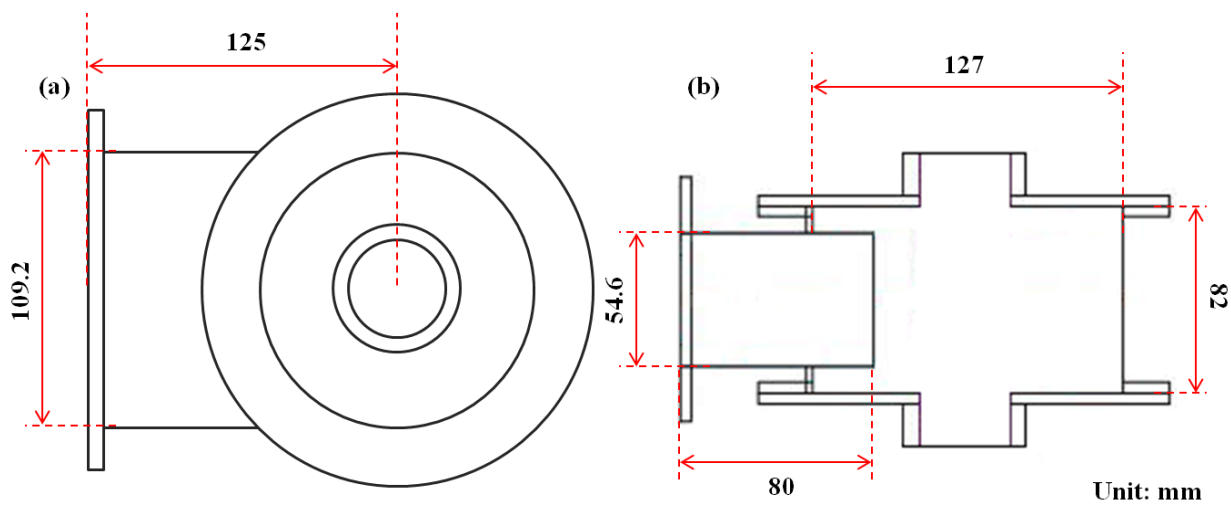

Figure 1. Schematic of the cylindrical microwave cavity resonator: (a) top view, and (b) side view.

the y direction and half variation in the x and z directions, the resonant frequency (f_r) could be calculated from the following equation:

$$f_r = \frac{c}{2\pi\sqrt{\mu_r \varepsilon_r}} \sqrt{\left(\frac{m\pi}{a}\right)^2 + \left(\frac{n\pi}{b}\right)^2 + \left(\frac{l\pi}{d}\right)^2} \quad (12)$$

where d is the length of the rectangular cavity resonator.

For estimating the height of the cylindrical cavity resonator, the resonant frequency (f_r = 2.32 GHz) determined from Eq. (12) was substituted into Eq. (11). The calculated height (82 mm) was used for designing the cylindrical cavity resonator. The cylindrical cavity resonator was made from stainless steel.

Rectangular waveguide

When two rectangular waveguides with different cross-sections need to be coupled, a gradual waveguide taper can be used to minimize the microwave power loss from the reflected wave (Kimura et al., 2009). In order to deliver high performance at high power levels, the taper length should be at least twofold the guide wavelength (λ_g) of the input rectangular waveguide. However, when there is no sufficient space to place the taper to connect the two waveguides, it is possible to directly couple the cross-sections of the input and output waveguides by maintaining the length of the input waveguide at 40 mm, which is almost a quarter of the wavelength for 2.45 GHz (Kimura et al., 2009). This coupling method could be applied to a microwave power system that requires high-energy transfer efficiency from the microwave energy to thermal energy (Cull and Carnahan, 1988). In addition, microwave power could be sequentially transmitted via a transition from the WR430 to WR284 waveguides (72.1 mm wide and 34.0 mm high) when a 2.45 GHz magnetron was used as a microwave power supply (Wheeler et al., 2002). Although the usable frequency range of the WR284 waveguide is between 2.60 and 3.95 GHz, this waveguide is frequently implemented for 2.45 GHz operation at the average power level of 6 kW (Kaur et al.). In this study, a WR284 rectangular waveguide that was 296 mm long ($2\lambda_g$ of the WR430 waveguide) and was built from nickel-coated brass, was used for transmitting high microwave power to the narrow cylindrical cavity.

With the dimensions of microwave power launcher, waveguide, and cylindrical cavity, the distribution of the electric field in the microwave heating chamber was simulated in three dimensions by using the COMSOL Multiphysics Software (COMSOL 4.3, COMSOL Inc., Palo Alto, CA). The electromagnetic field generated by the magnetron was determined by using the electromagnetic waves module with generalized minimal residual methods (GMRES). Electric field distributions in the microwave heating chamber and the cylindrical cavity are shown in Figure 2. More than 6 multiple hot spots are observed in the microwave power launcher and waveguide, and the electric field intensity peaked near the waveguide center. The presence of multiple hotspots could cause the loss of the heating efficiency at the cavity center and could damage the magnetron. Although the electric field was maximal on the central axis of the cylindrical cavity, the field strength did not reach the field strength required for

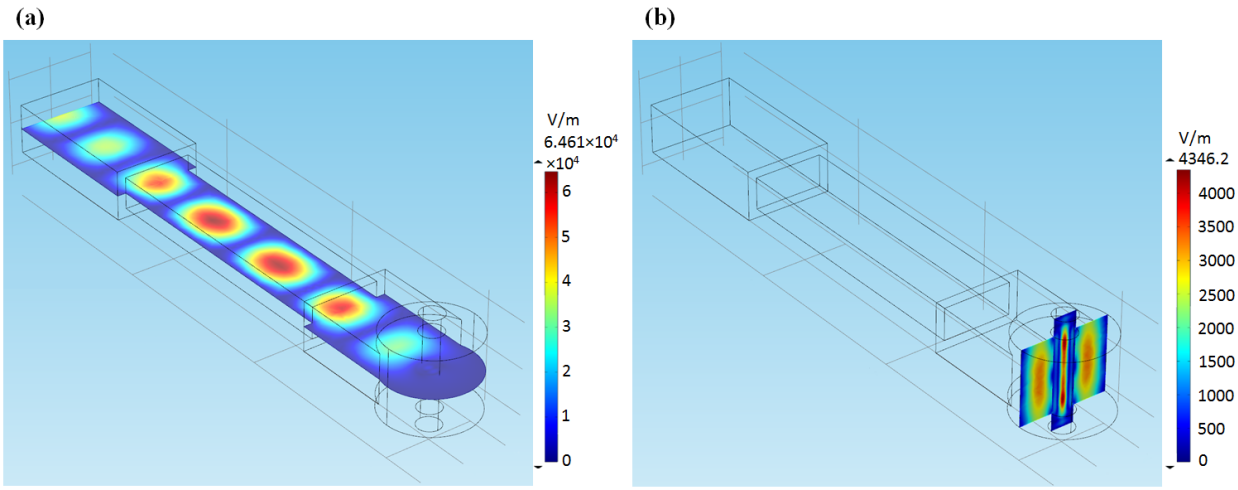

Figure 2. Electric field distributions in (a) the microwave heating chamber, and (b) the cylindrical cavity, before adjusting the position and inserting depth of the stubs.

the heating of multiphase foods (Figure 2(b)). Therefore, impedance matching had to be performed for achieving the maximal microwave power without wave reflection.

Impedance matching

The complex impedances between the load and the microwave power source should be matched to minimize the reflected wave and to protect the magnetron. In a microwave communication system, the distance between stubs can be determined depending on the guide wavelength (λ_g) as mentioned above; while the positions of the stubs on the microwave heating unit are often decided by trial and error (Chan and Reader, 2000). A common method for the impedance matching is to insert metallic rods or screws into the waveguide, with specific depth at certain locations; however, the lack of arrangement of the stubs on the waveguide could disable the entire microwave heating system. Therefore, prior to the fabrication of the developed microwave heating unit, the stubs on the designed power launcher, rectangular waveguide, and cylindrical cavity resonator were tuned in the computational COMSOL-based simulation. The 3D geometry of the microwave heating chamber was created by using the AutoCAD software (Autodesk Inc., San Rafael, CA) and was imported into the COMSOL interface (Figure 3). The tetrahedral mesh was used particularly owing to the shape of the ohmic chamber, and the computational domain was discretized into 38,140 mesh elements.

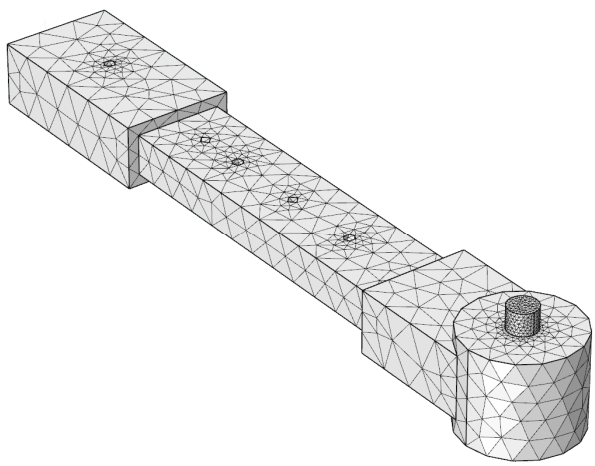

Figure 3. 3D geometry of the microwave heating chamber and the tetrahedral mesh.

After tuning the stubs in the simulation, the electric field distribution in the microwave heating cavity was also simulated and is shown in Figure 4. After performing the impedance matching, the multiple hotspots observed in Figure 2(a) were reduced and the desirable electric field strength was obtained in the microwave cavity (Figure 4(a)). The electric field strength simulated in the microwave heating cavity ranged from 2.245 to 5.649 kV/m (Figure 4(b)). A cross-sectional view of the chamber clearly indicates that the electric field is focused at the center and the maximal microwave power density is in the areas adjacent to the applicator's inlet and outlet. Based on the simulation results, the positions and inserting depths of the stainless steel stubs (diameter of 10 mm, height of 120 mm) were used in the fabrication of the microwave heating chamber.

The reflection coefficients (S_{11}) for the first and second microwave chambers (Figures 5(a) and 5(b)) that were needed for the dual microwave heating system were measured by filling the polytetrafuoreoethylene tube

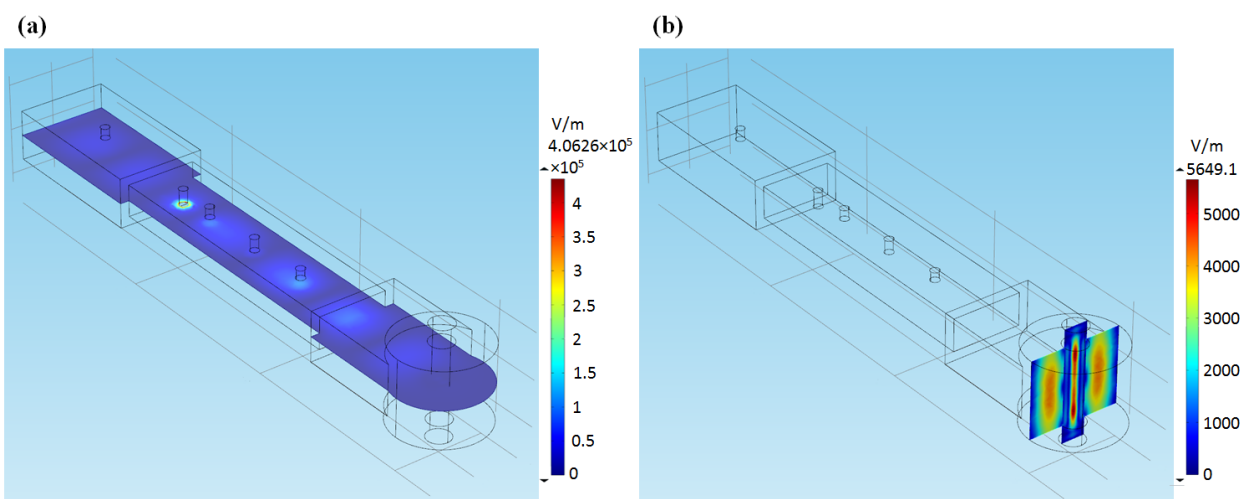

Figure 4. Electric field distributions in (a) the microwave heating chamber, and (b) the cylindrical cavity after inserting the stubs.

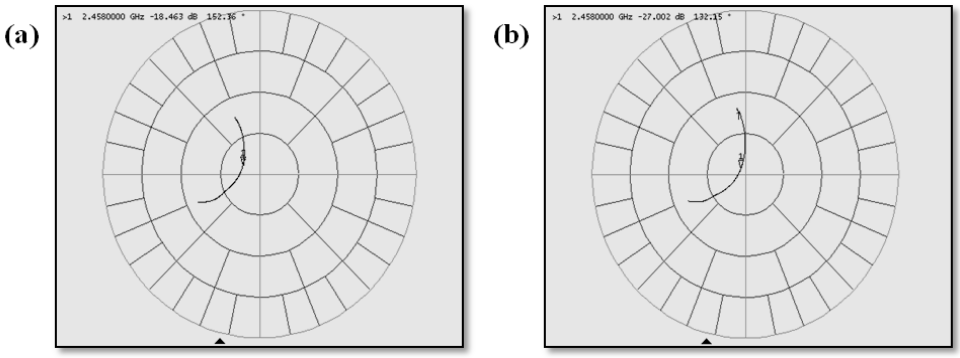

Figure 5. Impedance matching of (a) chamber 1 and (b) chamber 2. Smith charts show the reflection coefficient S_{11}, implying the characteristic impedance (Z_0) of 50 Ω.

(length - 190 mm, inner/outer diameter - 25.4/38.1 mm, Virgin electrical grade Teflon@ PTFE, Santa Fe Springs, CA) with water; the tube was used for the applicator and the coefficients were registered while adjusting the depths of 5 matching stubs. During the stub matching process, the marker indicating the value of S_{11} moved closer to the center of the Smith chart where the wave reflection is minimal (Figure 5). Return loss (R.L = 20 log S_{11} dB), corresponding to the loss of power delivery from a microwave generator to a load, was calculated by using the S_{11} value (Pozar, 2005). The values of S_{11} and return loss (dB) for the first and second chambers after the impedance matching were 0.12/-18.463 dB and 0.045/-27.002 dB, respectively. The results clearly imply that the magnetrons are not likely to be damaged by wave reflection, and the maximal microwave power could be transmitted to the working chambers. After performing the impedance matching, the test to determine the extent of microwave radiation leakage was performed for the developed microwave system by using a microwave leak detector (1074T2, McMaster-Carr, Elmhurst, IL, USA). No microwave radiation leakage was detected and the developed microwave heating system was found to be hermetically sealed.

Ohmic heating applicator

The ohmic and microwave combination applicators were fabricated by using two PTFE tubes (length - 190 mm, inner/outer diameter - 25.4/38.1 mm). Because the PTFE has a relatively low dielectric constant (~2.1) and is as transparent to microwaves as glass, the microwaves can penetrate the PTFE tube with negligible dielectric heating. Two titanium tubular electrodes (length - 25 mm, inner/outer diameter - 25.4/31.8 mm, Tico Titanium Inc., Wixom, MI) were placed at both ends of the PTFE tube. Titanium electrodes have demonstrated strong resistance to acidic conditions and low corrosion rate. In addition, electrolytic reactions, i.e., gas production and dissolution, rarely occur on titanium electrodes (Lima et al., 1999). Ohmic power supply based on an integrated gate bipolar transistor (IGBT, SKYPER™, SEMIKRON Inc., Hudson, NH) was used for the generation of alternating current with pulsed square waveform (maximal frequency of 20 kHz, on/off duty cycle of 0.2, max current of 100 A). A high-frequency pulsed square waveform can minimize the undesired electrochemical reactions occurring at the interfaces between the electrodes and food samples, because no electrons are present on the electrical double layers. A 190-mm-wide gap between the electrodes was the minimal required distance for preventing dielectric heating of the electrode surface by microwave.

The electric field distribution in the ohmic applicator was also simulated by using COMSOL. A conductive medium DC module with parallel direct sparse solver (PARDISO) was used to simulate the electric field distribution in the applicator. To predict the electric field distribution in multiphase foods subject to ohmic heating, the properties of solid particles were added to the simulation.

When the AC source voltage was 200 V, the estimated electric field strength ranged from 675.4 to 3650.2 V/m (Figure 6). Although a uniform electric field distribution was observed between ring-shaped electrodes, the electric field strength in the areas adjacent to top and bottom of solid particulates was relatively low, probably owing to the particles' field disruption (Shim et al., 2010). The electrical resistance (Ω) in those particular areas was relatively lower than that of solid particles and the majority of electrical current passed through highly conductive

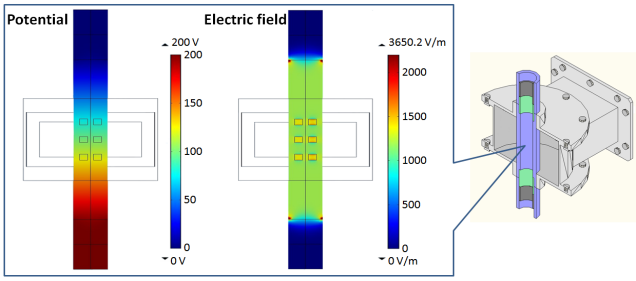

Figure 6. Electric field distribution in the ohmic heating applicator.

solution (Sastry and Palaniappan, 1992; Salengke and Sastry, 2007). Furthermore, localized field overshoots (approximately 3.6 kV/m) occurred at both edges of the electrodes. This phenomenon can result in numerous problems, such as the corrosion on the electrodes edges in a batch system; however, the overall performance of the heater in a continuous flow mode was not significantly influenced by the localized field overshoots because it occurred in a relatively small area.

Overall design of microwave and ohmic combination heater

Dual cylindrical microwave heating chambers were designed and fabricated to concentrate and resonate the electric field strengths from ohmic and microwave power sources (Figure 7(a)). The chamber had two ports connected to the waveguides that were built from nickel-coated brass, and 5 towers for microwave stub matching. Two magnetrons (2450 MHz; Model OM75S, Samsung), which could deliver up to 900 W each, were mounted at the end of each waveguide (Figure 7). One PTFE ohmic tube installed through the cavity was transparent to microwave, yielding negligible dielectric heating. Two titanium ring-shaped electrodes were placed at both ends of the ohmic heating tube (Figure 7(d)). The electrodes were connected to the power supply based on an integrated-gate-bipolar-transistor.

In addition, the effect of microwave and ohmic combination heater on uniform heating of multiphase foods was validated by using particle and liquid mixture foods that consisted of two fixed-size chicken breasts and potato cubes as well as base solutions mixed with sodium chloride and carboxymethyl cellulose (CMC) solutions, and NaCl solution with different salt concentration (Lee et al., 2015). When the particle and liquid mixture foods were treated by individual microwave and ohmic heating, the temperature difference between the particles and liquid foods was significant; however, uniform heating of

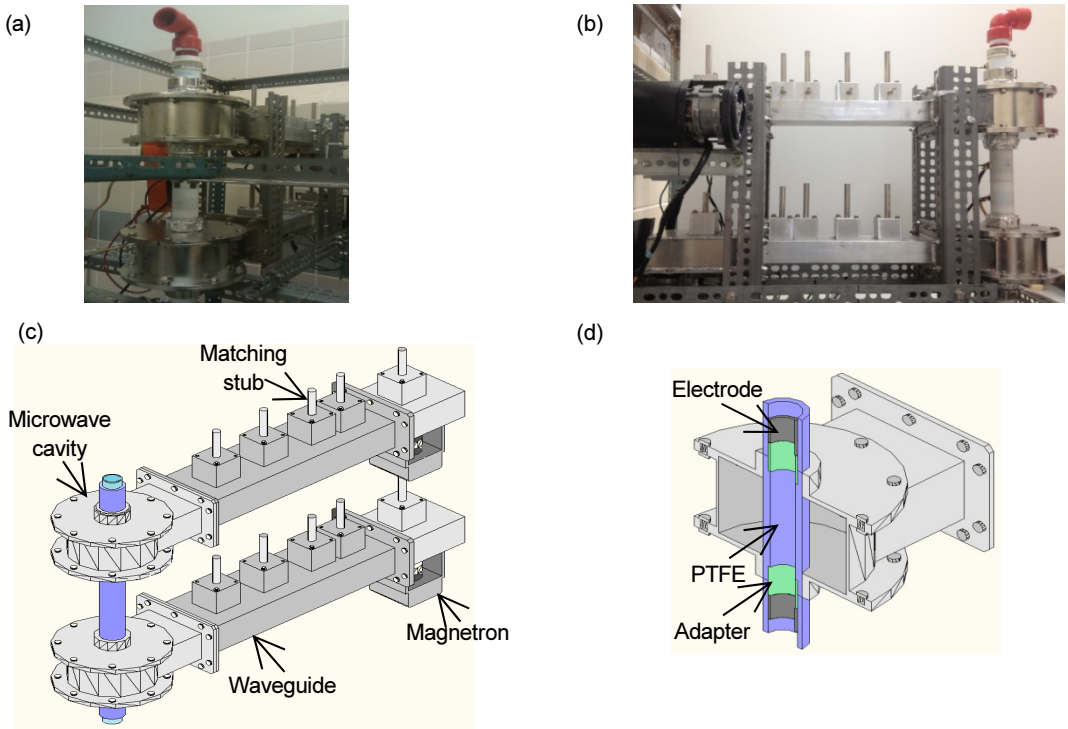

Figure 7. Schematic of the microwave and ohmic combination heater: (a) the front view, (b) a side view, (c) a 3D schematic, and (d) a cross-sectional view of the chamber.

particles and liquid mixture foods was obtained in the combination heating, finally resulting in a quite acceptable temperature difference between particles and liquid foods for commercial production of multiphase foods (Lee et al., 2015).

Conclusions

Single-mode cylindrical microwave cavity for the simultaneous microwave and ohmic combination heater was successfully designed and fabricated to achieve the maximal microwave power density at the central axis. All components comprising the designed microwave heating unit were suitable for transmitting maximal microwave power to the load. The simulated electric field distribution in the cavity indicated that single-mode microwave heating was likely to steadily generate highly localized heating zone in the cavity. In addition, the values of S_{11} (reflection coefficient) obtained from the impedance matching implied minimal power loss and wave reflection. In conclusion, the concentrated microwave power at the centerline under single-frequency microwave method would be beneficial for thermal treatment of multiphase foods without attenuating the microwave power.

Conflict of Interest

The authors have no conflicting financial or other interests.

Acknowledgments

This project was supported by Agriculture and Food Research Initiative Grant 2009-65503-05786 from the USDA, National Institute of Food and Agriculture.

References

Anantheswaran, R. C. and L. Liu. 1994. Effect of viscosity and salt concentration on microwave heating of model non-Newtonian liquid foods in a cylindrical container. Journal of microwave power and electromagnetic energy 29(2):119-126.

Barlow, S. and S. R. Marder. 2003. Single-mode microwave synthesis in organic materials chemistry. Advanced Functional Materials 13(7):517-518.

Berliner, L. and C. Bender. 2004. EPR: Instrumental Methods (No. 21). Springer Science and Business Media.

Bradshaw, S. M., E. J. Van Wyk and J. B. De Swardt. 1998. Microwave heating principles and the application to the regeneration of granular activated carbon. Journal of the South African Institute of Mining and Metallurgy (South Africa) 98(4):201-210.

Chan, T. V. C. T. and H. C. Reader. 2000. Understanding microwave heating cavities, pp. 25-40. London, UK: Artech House Publishers.

Cha-um, W., P. Rattanadecho and W. Pakdee. 2009. Experimental analysis of microwave heating of dielectric materials using a rectangular wave guide (MODE: TE 10)(case study: water layer and saturated porous medium). Experimental Thermal and Fluid Science, 33(3):472-481.

Chen, L. F., C. K. Ong, C. P. Neo, V. V. Varadan and V. K. Varadan. 2004. Microwave electronics: measurement and materials characterization, pp. 36-45, New Jersey, USA: John Wiley and Sons.

Cooper, R. K. and R.G. Carter. 1991. High power RF transmission. In Proceedings of the CERN Accelerator School: RF Engineering for Particle Accelerators, pp. 92-103. Oxford, UK.

Cull, K. B. and J. W. Carnahan. 1988. Design considerations and preliminary characterizations of a kilowatt-plus microwave-induced plasma. Applied spectroscopy, 42(6):1061-1065.

Das, S., A. K. Mukhopadhyay, S. Datta and D. Basu. 2009. Prospects of microwave processing: an overview. Bulletin of materials science 31(7):943-956.

De Alwis, A. A. P. and P. J. Fryer. 1990. A finite-element analysis of heat generation and transfer during ohmic heating of food. Chemical Engineering Science 45(6): 1547-1559.

Elashafiey, T. M. F. 2011. Simple novel qualitative approach for electromagnetic wave analysis of rectangular waveguides without usage of Maxwell's equations. Paper presented at the IEEE Symposium on Wireless Technology and Applications (ISWTA).September, pp. 25-28.

Hardy, W. N. and L. A. Whitehead. 1981. Split-ring resonator for use in magnetic resonance from 200-2000 MHz. Review of Scientific Instruments 52(2):213-216.

Kaur, J., M. Saini. R. Singh and K. Singh Performance

Improvements in Microwave Wave Guide.

Kimura, Y., H. Kawaguchi, S. Kagami, M. Furukawa and H. Shindo. 2009. A New Method of Line Plasma Production by Microwave in a Narrowed Rectangular Waveguide. Applied Physics Express 2(12):126002.

Kybartas, D., E. Ibenskis and R. Surna. 2011. Single Mode Circular Waveguide Applicator for Microwave Heating of Oblong Objects in Food Research. Elektronika ir Elektrotechnika 114(8):79-82.

Lee, S. H. and S. Jun. 2011. Enhancement of sugar release from taro waste using ohmic heating and microwave heating techniques. Transactions of the ASABE 54(3): 1041-1047.

Lee, S. H., W. Choi, C. T. Kim and S. Jun. 2015. Development of a dual cylindrical microwave and ohmic combination heater for minimization of thermal lags in the processing of particulate foods. LWT-Food Science and Technology 63(2):1220-1228.

Lima, M., B. F. Heskitt, L. L. Burianek, S. E. Nokes and S. K. Sastry. 1999. Ascorbic acid degradation kinetics during conventional and ohmic heating. Journal of Food Processing and Preservation 23(5):421-443.

Mekis, A., J. C. Chen, I. Kurland, S. Fan, P. R. Villeneuve and J. D. Joannopoulos. 1996. High transmission through sharp bends in photonic crystal waveguides. Physical Review Letters 77(18):3787-3790.

Nguyen, L. T., W. Choi, S. H. Lee and S. Jun. 2013. Exploring the heating patterns of multiphase foods in a continuous flow, simultaneous microwave and ohmic combination heater. Journal of Food Engineering 116(1):65-71.

Pozar, D. M. 2005. Microwave engineering, 3rd Ed., pp. 106-125, 174-183, and 283-285. Wiley, Danvers, MA.

Rattanadecho, P., N. Suwannapum, B. Chatveera, D. Atong and N. Makul. 2008. Development of compressive strength of cement paste under accelerated curing by using a continuous microwave thermal processor. Materials Science and Engineering A, 472(1):299-307.

Roussy, G. and J. A. Pearce. 1998. Foundations and industrial applications of microwaves and radio frequency fields. Physical And Chemical Processes. In Optimization of Electrical and Electronic Equipments, 1998. OPTIM'98. Proceedings of the 6th International Conference on (Vol. 1, pp. 115-116). IEEE.

Salengke, S. and S. K. Sastry. 2007. Experimental investigation of ohmic heating of solid–liquid mixtures under worst-case heating scenarios. Journal of food engineering 83(3):324-336.

Sastry, S. K. and S. Palaniappan. 1992. Mathematical modeling and experimental studies on ohmic heating of liquid-particle mixtures in a static heater. Journal of Food Process Engineering 15(4):241-261.

Shim, J., S. H. Lee and S. Jun. 2010. Modeling of ohmic heating patterns of multiphase food products using computational fluid dynamics codes. Journal of food engineering 99(2):136-141.

Sreekanth, P. V. 2003. Digital Microwave Communication Systems: With Selected Topics in Mobile Communications. Universities Press.

Sun, R., L. C. Kempel, L. Zong, S. Zhou and M. C. Hawley. 2005. Electromagnetic modeling of an adaptable multimode microwave applicator for polymer processing. Applied Computational Electromagnetics Society Journal 20:43-48.

Tang, X. W., S. J. Jiao, Z. Y. Gao and X. L. Xu. 2008. Study of 5.8 GHz magnetron in microwave deicing. Journal of Electromagnetic Waves and Applications 22(10): 1351-1360.

Torungrueng, D. and C. Thimaporn. 2004. A generalized ZY Smith chart for solving nonreciprocal uniform transmission-line problems. Microwave and Optical Technology Letters 40(1):57-61.

Tran, V. N. 1992. An applicator design for processing large quantities of dielectric material. PhD thesis. Eakin University Victoria, Burwood VIC, Australia.

Veronis, G. and S. Fan. 2005. Bends and splitters in metal-dielectric-metal subwavelength plasmonic waveguides. Applied Physics Letters 87(13):131102.

Wheeler, R. R., J. E. Atwater, J. R. Akse, J. T. Holtsnider and B. Luna. 2002. Development and Testing of a Microwave Powered Regenerable Air Purification Technology Demonstrator (No. 2002-01-2403). SAE Technical Paper.

Zhao, X., L. Yan and K. Huang. 2011. Review of numerical simulation of microwave heating process. In *Advances in Induction and Microwave Heating of Mineral and Organic Materials*, (S. Grundas, eds) pp. 27-48, Rijeka, Croatia.